Neural Network-Based Receiver in Band-Limited Communication System with MPPSK Modulation

Zixin Wang[1], *Fan* Meng[1,*], and *Lenan* Wu[1]

[1] School of Information Science and Engineering, Southeast University, Nanjing 210096, China

Abstract. As a type of the spectrally efficient modulation, the m-ary phase position shift keying (MPPSK) has been considered to meet the increasing spectrum requirement in the future wireless system. To limit the signal bandwidth and cancel the out-band interference the band-pass filters are used, which introduce the waveform distortion and inter-symbol interference (ISI). Therefore, a single hidden-layer neural network (NN)-based receiver is proposed to jointly equalize and demodulate the received signal. The impulse response of the system is static and the network parameters can be obtained after off-line training. The number of the hidden nodes is also determined through simulations. Simulation results show that the NN-based receiver works well in the communication system with different allocated bandwidths. By observing the modified confusion matrix, the false symbol decision is relevant to modulation index, waveform distortions and the ISI.

1 Introduction

To satisfy the fast-growing broadband wireless service, more high-speed transmission of information within the unit band is required. Since the frequency resources are valuable, a class of efficient modulation techniques named as "Ultra Narrow Band (UNB)" has been concerned [1-4]. Based on the extended binary phase shift keying (EBPSK) [5], an m-ary phase position shift keying (MPPSK) modulation is considered as a multi-level form of EBPSK.

In the wireless communication systems, the band-pass infinite impulse response (IIR) filters [6,7], which have less orders than the FIR filters to satisfy the same specifications, are adopted to suppress the sidelobe of the transmitted signal and eliminate the out-band interference at both the transmitter and receiver. Meanwhile, the waveform distortion, the inter-symbol interference (ISI) of adjacent symbols and the band-pass Gaussian noise can be caused by the IIR filters. Therefore, in that case the traditional demodulation methods based on matched filter (MF) [8] or impacting filter [9, 10] cannot work well. To solve these problems, the following two modules can be adopted: 1) an equalization to reduce the confirmed ISI; 2) a MF to match the distorted waveform. However, the communication system is usually assumed to be FIR rather than IIR for the traditional equalization methods

[*]Corresponding author: mengxiaomaomao@outlook.com

[11,12]. In addition, the received signal is filtered symbol by symbol instead of at a sampling interval, and the computational complexity increases with more orders (up to several dozen) of the equalization.

The neural network (NN) [13], which has been successfully applied in many scenarios such as control engineering [14], computer vision [15] and recently communication engineering [16,17]. With its remarkable capacity to infer the mapping implied by the training data, we propose a single hidden- layer NN-based receiver. The joint equalization and demodulation task can be finished by a single NN-based receiver. Since the impulse response of the system is static, the network parameters can be obtained through off-line training with large amount of data. The number of the hidden nodes is also determined through simulations. The simulation results show that the NN-based receiver can overcome the waveform distortions and ISI in a single network. Besides, by observing the modified confusion matrix, the false symbol decision can be mainly attributed to ISI, especially in the region of higher SNR. The waveform distortions also decrease the constellation point distance, which means the system requires higher SNR to obtain the same SER.

The rest of this paper is organized as follows. Section 2 introduces the system model of a band- limited wireless communication. In Section 3, we introduce the structure of a single hidden-layer feed-forward NN (FNN), hyper-parameter settings of the network and the input/output data. Then, in Section 4, the single-layer NN-based receiver is tested and the simulation results are analyzed. Conclusions and discussion are given in Section 5.

2 System model

The MPPSK modulation [18] is considered with the symbol guard interval factor being $r_g = 0$ and the phase shift being $\theta = \pi$, respectively. Finally, for symbol $m \in \{1, \cdots, M\}$, the modulated MPPSK signal is written as

$$g^m(t) = \begin{cases} \sin(2\pi f_c t) & 0 \le t < (m-1)KT_c \\ -\sin(2\pi f_c t) & (m-1)KT_c \le t < mKT_c \\ \sin(2\pi f_c t), & mKT \le t < NT_c \end{cases} \quad (1)$$

where $T_c = 1/f_c$ denotes the carrier period. K and N represent the number of carrier periods in each time slot and in each symbol, respectively. Apparently, we have $N = KM$ and $T = NT_c$, where T denotes the MPPSK symbol duration. The diagram of a wireless band-limited communication system used in our paper is shown in Fig. 1.

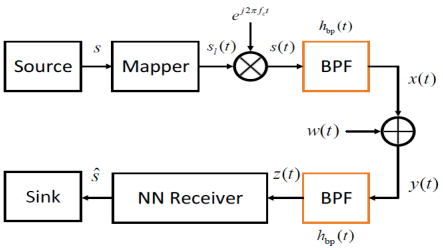

Fig. 1. The diagram of the band-limited communication system

The symbol sequence s is produced from the source, and mapped into a baseband signal $s_l(t)$, which can be represented as

$$s_l(t) = \sum g_n(t - nT), \tag{2}$$

where $g_n(t) \in G = \left\{ g^1(t), \cdots, g^M(t) \right\}, n \in \mathbb{N}$.

Then $s_l(t)$ is up-converted into the band-pass signal $s(t) = s_l(t)e^{j2\pi f_c t}$ by the carrier frequency f_c, and it is shaped by a bandpass filter. Finally, the transmitted signal is denoted as

$$x(t) = s(t) * h_{bp}(t), \tag{3}$$

where the $*$ represents convolution operator and $h_{bp}(t)$ denotes the impulse response of the filter. The channel impulse response is assumed to be $\delta(t)$ and $w(t)$ is the additive white Gaussian noise (AWGN) with zero mean and variance σ_w^2. Then the received signal $y(t)$ can be described as $y(t) = x(t) + w(t)$.

At the transmitter, a same passband filter is used to reduce the out-band interference. Signal $z(t)$ after the passband filter is obtained as:

$$z(t) = y(t) * h_{bp}(t) = s''(t) + w'(t). \tag{4}$$

The notation $s''(t)$ represents that the signal $s(t)$ is filtered twice, and noise $w'(t)$ is filtered once.

The task is to equalize and demodulate the band-limited signal. Since the band-pass filter is used, the waveform distortion and ISI are introduced. A MF corresponding to the distorted symbol waveform can be designed by a NN-based method. The convoluted signal also can be equalized by a NN-based module. Moreover, the function of the two modules working as the MF and the equalizer separately can be realized by a single NN-based module. The NN-based receiver can jointly equalize and demodulate the signal and directly produce the estimated symbol sequence $\hat{s}$.

3 NN-based receiver

The core part of the NN-based receiver is a FNN. Generally, it is a composition of one input layer, L hidden layers and one output layer of computational units [19]. Particularly, the single-hidden layer $(L = 1)$ NN is considered in our paper, which is illustrated in Fig. 2.

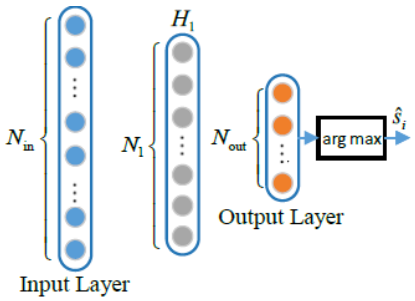

Fig. 2. The schematic diagram of a NN-based receiver

3.1 Feed-forward neural network

A mapping function $F_{\text{FNN}} : R_{\text{in}}^{N} \Rightarrow R_{\text{out}}^{N}$ of FNN is defined as:

$$F_{\text{FNN}}(\mathbf{x};\theta) = g_{\text{out}}\, o f_{\text{out}}\, o g_1\, o f_1\, o(\mathbf{x})^{\circ} \tag{5}$$

where $\mathbf{x}$ denotes the input vector, $f_1\, o$ denotes a linear pre-activation function and $g_1 \circ$ denotes a nonlinear activation function of the hidden layer. The activation of the input layer is linear. The parameter θ is composed of weight matrix $\mathbf{W}_1 \in R^{N_1 \times N_{\text{in}}}$ and bias vector $\mathbf{b}_1 \in R^{N_1}$, and the $\mathbf{W}_{\text{out}}$, $\mathbf{b}_{\text{out}}$ of output layer are also included. The output of the hidden layer is vector $\mathbf{x}_1 = [x_{1,1}, \cdots, x_{1,N_1}]^T$, it is computed from the activations of the preceding layer, i.e. the input layer. Given the input vector $\mathbf{x}$, the pre-activation of the hidden layer is given as

$$f_1(\mathbf{x}) = \mathbf{W}_1\mathbf{x} + \mathbf{b}_1. \tag{6}$$

After the corresponding non-linear activating nodes, the output of the hidden layer can be written as

$$\mathbf{x}_1 = g_1(f_1(\mathbf{x})), \tag{7}$$

where the activation functions g1 used in FNN are all rectified linear unit (ReLU) [20], which is $g(x) = \max(0, x)$. It is shown that ReLU is much faster than widely used sigmoid in terms of calculation speed [21]. Besides, there is no nonlinearity in this task and extra nonlinear approximation capability is unnecessary.

3.2 Data and hyper-parameters

The input vector $\mathbf{x}$ for the corresponding symbol s_i to be inferred is composed of a piece of windowed sampled received signal $z(n)$. Considering the convoluted signal, the window size is set larger than one symbol interval. Meanwhile large window can introduce a large amount of uncorrelated data, which can make the training process hard to converge. Therefore, a window of medium size is proposed. The size of input vector is denoted by N_{in}, and it can be written as:

$$N_{\text{in}} = N \times N_s \times f_s / f_c, \tag{8}$$

where N_s represents the corresponding normalized window size (divided by symbol duration). More concretely, the sampled data of $N_s = 1.25$ successive symbols is used in our simulations. The parameters of MPPSK modulation is list as follows: $M = 64, K = 4$. The carrier frequency is $f_c = 70$ MHz and the sampling frequency is $f_s = 280$ MHz. Therefore the final N_{in} is 1280.

This is a classification problem to classify the convoluted signal with colored noise. By assigning a generalization of the logistic function, i.e. soft-max activation function [22] for categorical target variables $(M > 2)$, the number of target variables $N_{\text{out}} = M$ for classification. The output of softmax activation function g_{out} is $\mathbf{y} = [y_1, \cdots, y_M]^T$, and the element y_i is defined as:

$$y_i = \frac{e^{x_i}}{\sum_{j=1}^{M} e^{x_j}} \tag{9}$$

where x_j is j-th unit output of previous layer, i.e the last hidden layer. The estimation $\hat{s}_i$ can be obtained by selecting the maximal element in the output vector, which is shown in Fig. 2.

Since $N_{\text{in}} = 1280$, the input dimension is very high and serious over-fitting can be introduced in the training process. Therefore a callback is proposed in the training process. The validation loss is stored after each training epoch and finally the network parameter θ with the lowest loss is loaded in the NN-based receiver. The loss function is cross-entropy error minimizing, and it is optimized by Adam algorithm [23] with default settings. Besides, the detailed network and training settings are list in Tab. 1 and the parameter will be particularly mentioned if modified.

Table 1. Simulation parameters

Variables	Values
Number of Train Samples	9×10^4
Number of Validation Samples	1×10^4
Epoch Number for Network	20
Batch Size	128
Active Function	ReLU

There are several advantages on NN-based methods. Firstly, the whole system is time-invariant and the impulse response is known, which means plenty of training data can be easily obtained by simulations. Secondly, the accuracy of inference can be easily adjust by changing the network scale, which means the design of the NN-based receiver is flexible. Lastly, the NN can realize the functions of equalizer and demodulator in a single module, which simplifies the receiver design. Therefore, the receiver based on NN is used in the following simulation section.

4 Simulation results

After MPPSK modulation, the main lobe of the signal is up to 35 MHz, while the allocated bandwidth B = 10 MHz as shown in Fig. 3. This communication system is a wide band transmitting system.

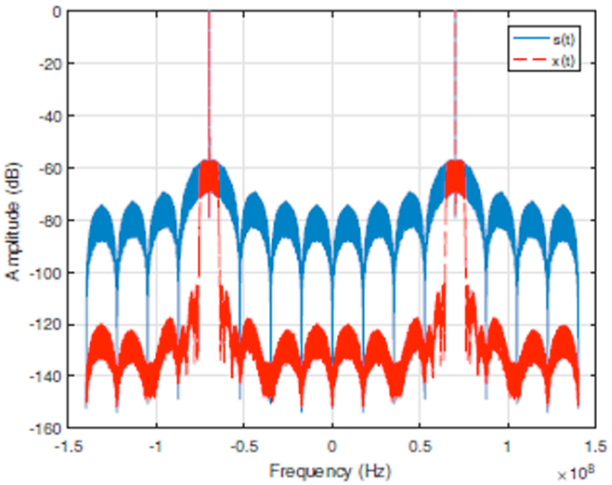

Fig. 3. PSD of the transmitted signals before and after the band-pass filter (B = 10 MHz)

For the bandpass filter (Chebyshev type II), the maximum passband ripple is $R_p = 3\text{dB}$, the minimum stopband attenuation is $R_s = 45\text{dB}$, and the frequency interval $\Delta f = 2\text{MHz}$. The normalized power spectrum densities (PSD) of the received signals after and before the bandpass filter are shown in Fig. 3. The sidelobe of $x(t)$ is sharply filtered to lower than 105dB compared to band MPPSK signal $s(t)$ is about -57dB. Under these parameters, the order of designed band-pass filter is 21.

4.1 Number of hidden nodes

We begin by comparing the performance of different numbers of hidden nodes N_h. The increasement of N_h can enhance the approximation ability of the network, while it requires greater computations and complexity of the receiver. The fast processing speed is more important under high transmitting symbol rate. Therefore we need to find a suitable size of network first, taking account of both performance and efficiency. The bandwidth is B = 10 MHz, and the training data, validation data and testing data are all the same to different networks.

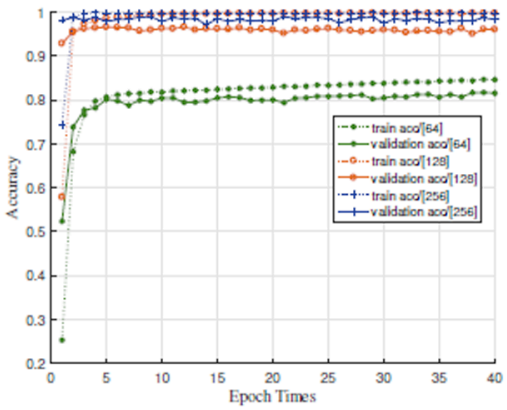

Fig. 4. Training and validation accuracy of different networks

The network of single-hidden layer is considered in this simulation, and $\{64\}$, $\{128\}$ and $\{256\}$ nodes, which are all integer multiples of *M*. In Fig. 4 the curves of accuracy and cross-entropy loss in training process are plotted. After about 5 epoch times, all validation loss and accuracy go stable with small jitters, while training accuracy remains rising and training loss keeps declining. This over-fitting issue can be solved by a callback, which selecting the best model parameters corresponding to the least validation loss in all training epochs.

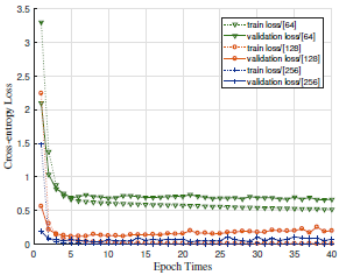

Fig. 5. SER/SNR curves of different numbers of hidden nodes (*B* = 10MHz)

As the nodes increases, the convergence values of validation accuracy increase, which are 0.85, 0.96 and 0.98 for N_h = 64, 128 and 256 in Fig. 4(a). Generally the trend of variation has an inverse relation with its corresponding loss, and therefore the values of loss decrease as the accuracy rise when comparing Fig. 4(a) and Fig. 4(b).

The SER/SNR curves of networks of different N_h are shown in Fig. 5. The SER performance of {64} nodes is poor, which can only achieve about 3.5×10^{-3} when SNR = 8dB. Meanwhile the network of $\{256\}$ nodes can obtain about 2.7×10^{-5}. In the region of SER=1.0×10^{-4}, the network of $\{256\}$ nodes can achieve about 1.4 dB gain over the $\{128\}$ nodes. In summary, the network of $\{256\}$ nodes works the best of all networks and we use it in the following simulations.

4.2 Bandwidth

In this subsection the bandwidth *B* is considered, while the other parameters remain as before. The bandwidths are set to be $B=\{6,10,20\}$MHz, and the corresponding training data is collected with SNR regions $\{[14,18],[6,8],[-2,0]\}$ dB. The simulation results are illustrated in Fig. 6. Generally it can be seen that as the bandwidth decreases, the SER performance of the NN-based receiver degrades with a higher value and a slower downward trend.

There is about 4.2 dB SNR gain to achieve the same SER = 1.0×10^{-3} when comparing curves of *B* = 10 MHz and *B* = 20 MHz. Moreover, the SNR gap goes larger as the SER decreases, and up to about 6.5 dB in the region of SER= 5.0×10^{-5}. As for the curve of allocated bandwidth is only *B* = 6 MHz, the SER is much poorer than the other two considering the more serious ISI.

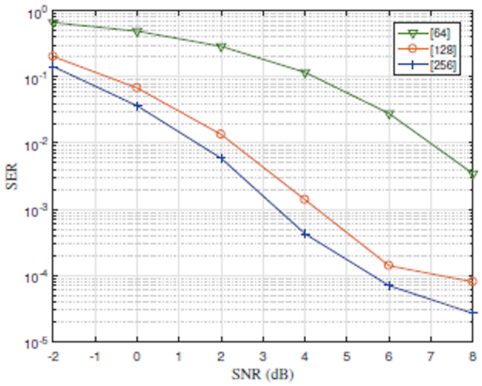

Fig. 6. SER/SNR curves of different numbers of hidden nodes(*B*=10 MHz)

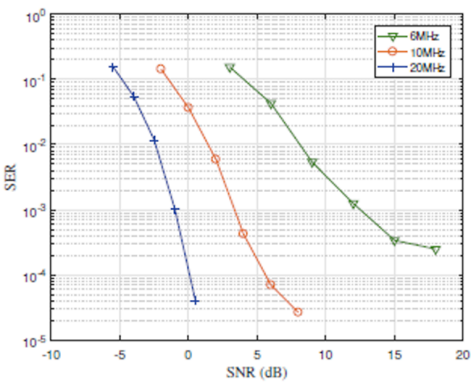

Fig. 7. SER/SNR curves under different bandwidth

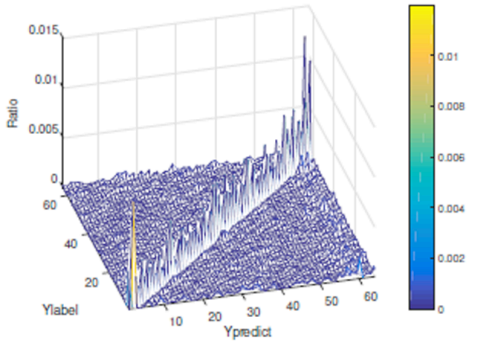

Fig. 8. A 3-D normalized conditional SER illustration when SNR=0 dB

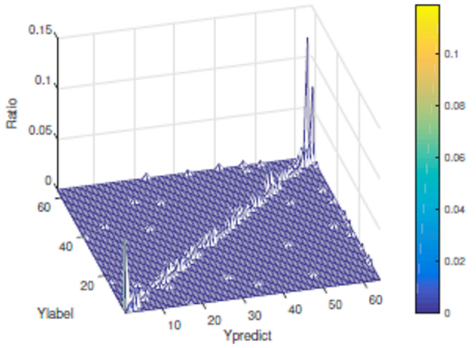

Fig. 9. A 3-D normalized conditional SER illustration when SNR = 4 dB

To further study the reasons for the symbol error, the modified confusion matrix is plotted in Fig. 7. The x-axis, y-axis, z-axis represents the estimated symbol labeled as Ypredict, the true symbol labels as Ylabel and the joint symbol error ratio R, respectively. The notation $R_{i,j}$ denotes the joint symbol error ratio for the pair of the estimated symbol $i \in \{1,\cdots,M\}$ and the true symbol $j \in \{1,\cdots,M\}$. We set $R_{i,j} = 0$ when $i = j$, to make the modified confusion matrix show only the error information, and the R can be normalized with $\sum_{i,j} R_{i,j} = 1$.

Firstly by observing Fig. 8 and Fig. 9, most errors occur at the neighborhood regions of $i, j = 1$ and $i, j = M$, whose locations of changing phase are at the fore-end and the back-end of the waveform. These errors are introduced by interference of the nearby symbols. Secondly, at the region of $|i - j| = 1$ the errors are easily introduced and the $R_{i,j}$ remains a constant when SNR is set. As the (1) shows that the MPPSK modulates the signal by locations of changing phase. The use of filters smooths the waveform of the signal, but it also aggravates the vagueness of the location information, which means the constellation point distance decreases. This type of mistakes can be reduced by increasing SNR. Lastly, all the other errors are caused by the noise and their probabilities remains a constant at a given SNR region.

5 Conclusions

The equalization and demodulation problem for MPPSK signals in a band-limited communication system with IIR filters at both the transmitter and receiver has been investigated. We propose a NN-based receiver and introduce its diagram and training process. The NN-based receiver works well under different bandwidth limitations with a single-hidden layer of 256 nodes. After inference result analysis, we find that the false symbol decision is relevant to modulation index m and can be attributed to ISI and waveform distortions. In the future work, more complex communication scenarios will be considered for the efficiently modulated signals.

Acknowledgments: This work was supported in part by the Fundamental Research Funds for the National Natural Science Foundation of China (Grant No. 61271204), and the SAST (Grant No. SAST2016071).

References

1. L. Wu, "UNB modulation in high speed space communications," Proc. of ICSIT, **6795**, 679 (2007)
2. M. Feng, L. Wu, "Special non-linear filter and extension to Shannon's channel capacity," Digital Signal Processing, **19**, 5, (2009)
3. M. Feng, L. Wu, P. Gao, "From special analogous crystal filters to digital impacting filters," Academic Press, Inc. (2012)
4. C. Lu, L. Wu, P. Chen, J. Wang, "M-ary phase position shift keying with orthogonal signalling," IET Communications, **9**, 12, (2015)
5. L. Wu, M. Feng, "On BER performance of EBPSK-MODEM in AWGN channel," Sensors, **10**, 4, (2010)
6. P. P. Vaidyanathan, P. Regalia, S. K. Mitra, "Design of doublycomplementary IIR digital filters, using a single complex allpass filter," *in Acoustics, Speech, and Signal Processing, IEEE Interna- tional Conference on ICASSP*, (1986)
7. A. V. Oppenheim, R. W. Schafer, "Discrete-time signal processing," **23**, 2, (1989)
8. C. Qi, L. Wu, "Pll demodulation technique for m -ray position phase shift keying," Journal of Electronics (China), **26**, 3, (2009)
9. L. Wu, H. Feng, "Extended binary phase shift keying modulation and demodulation method for frequency spectrum compression," (2009)
10. Z. Chen, L. Wu, P. Chen, "Efficient modulation and demodulation methods for multi-carrier communication," IET Communications, **10**, 5, (2016)
11. J. G. Proakis, M. Salehi, *Digital Communications.* (New York: McGraw-Hill, 1995)
12. C. A. Belfiore, J. Park, John H, "Decision feedback equalization," Proceedings of the IEEE, **67**, 8, (1979)
13. P. E. Keller, *Artificial Neural Networks: An Introduction* (2005)
14. H. Wei, H. Huang, S. S. Ge, "Adaptive neural network control of a robotic manipulator with time-varying output constraints," IEEE Transactions on Cybernetics, **47**, 10, (2017)
15. A. Krizhevsky, I. Sutskever, G. E. Hinton, "Imagenet classification with deep convolutional neural networks," in International Conference on Neural Information Processing Systems, (2012)
16. P. A. Haigh, Z. Ghassemlooy, I. Papakonstantinou, S. Rajbhandari, "Online artificial neural network equalization for a visible light communications system with an organic light emitting diode based transmitter," in Network and Optical Communications, (2013)

17. O. B. Belkacem, R. Zayani, M. L. Ammari, R. Bouallegue, D. Roviras, "Neural network equal- ization for frequency selective nonlinear mimo channels," in Computers and Communications, (2012)
18. P. Ying, L. Wu, "New scheme of MPPSK modem," Journal of Southeast University, (2012) Abramson2006Pattern
19. V. Koltchinskii, "Neural network learning: Theoretical foundations," Annales De L Institut Henri Poincare Probabilites Et Statistiques, **39**, 6, (2003)
20. X. Glorot, A. Bordes, Y. Bengio, "Deep sparse rectifier neural networks," in International Con- ference on Artificial Intelligence and Statistics, (2011)
21. Y. LeCun, Y. Bengio, G. Hinton, "Deep learning," Nature, **521**, 7553, (2015)
22. N. Abramson, D. Braverman, G. Sebestyen, *Pattern recognition and machine learning.* (Springer, 2006)
23. D. P. Kingma, J. Ba, "Adam: A method for stochastic optimization," Computer Science, (2014)